ROYAL SOCIETY
OF CHEMISTRY

PAPER

Check for updates

Utilizing an attritor mill for solvent-free mechanochemical synthesis of *rac*-ibuprofen:nicotinamide co-crystals

Sarah Triller, Frederik Winkelmann, Jan-Hendrik Schöbel [ID] and Michael Felderhoff [ID] *

The co-crystal formed from the WHO essential drug *rac*-ibuprofen (IBU) and the food additive nicotinamide (NIC) exhibits enhanced physicochemical and analgesic properties compared to the pure active pharmaceutical ingredient (API), exemplifying how co-crystallization can modify pharmaceutical characteristics. Herein, we present a more sustainable, solvent-free mechanochemical process for synthesizing *rac*-ibuprofen:nicotinamide (IBU:NIC) co-crystals, moving beyond conventional solution-based methods that typically require substantial amounts of solvents and energy. For the first time, we investigate the application of a horizontal attritor mill for co-crystal synthesis. Our findings demonstrate the effectiveness of this milling technology in facilitating the co-crystallization process, achieving pure co-crystals within 30 min. Additionally, initial experiments were conducted to explore the transition from a batch process to a sequential process. While our approach demonstrate the use of attritor mills for pharmaceutical co-crystal synthesis on a multigram scale, it also indicates opportunities for scaling up this process using industrial attritor mills. This work underscores the adaptation of existing grinding technologies to facilitate mechanochemical reactions, showcasing greener alternatives for pharmaceutical manufacturing.

Introduction

The formulation of an active pharmaceutical ingredient (API) into a co-crystal with a suitable coformer[1–3] has proven to be a valuable strategy for enhancing the mechanical and chemical stability,[4–6] as well as the physicochemical properties of pharmaceuticals.[7–9] Consequently, well-designed co-crystals can enhance the overall safety profile of the final drug compound. For example, the *rac*-ibuprofen:nicotinamide (IBU:NIC) co-crystal exhibit improved solubility and an increased analgesic effect compared to the parent drug.[10–12]

The synthesis of these co-crystals can be performed under mechanochemical conditions,[6,13–19] offering a safer and more environmentally friendly alternative to solution-based methods by significantly reducing solvent consumption and CO_2 emissions.[20–26] Considering that 80–90% of pharmaceutical waste consists of solvents,[27,28] this technology has significant potential to contribute to greener pharmaceutical manufacturing and achieving the United Nations Sustainable Development Goals (UN SDGs).[29] However, the technologies explored for conducting pharmaceutical co-crystal synthesis on an industrial scale are limited.[18,30–33] Recently, we reported on

the mechanochemical kilogram-scale synthesis of IBU:NIC co-crystals in batch processes using an eccentric vibratory mill[34] and a drum mill.[35] Alongside these technologies, the attritor mill, another milling device designed for the fine grinding of materials, presents a promising option for performing and scaling up mechanochemical transformations.

The attritor mill typically features a robust outer casing that encloses a horizontal or vertical cylindrical grinding chamber, along with an internal rotating shaft to provide the necessary
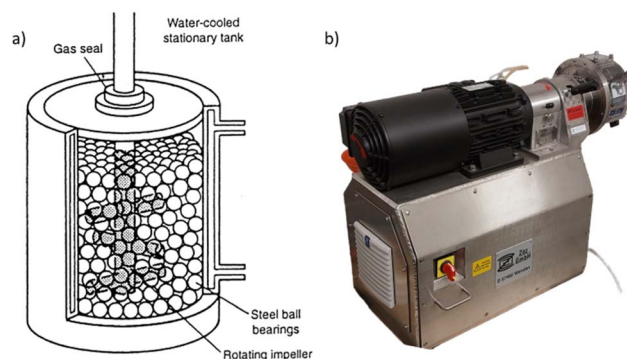

Fig. 1 (a) Schematic representation of a vertical attritor mill (reproduced with permission from Elsevier) and (b) horizontal attritor mill (Simoloyer CM01 from Zoz GmbH) used in this study.

Department of Heterogeneous Catalysis, Max-Planck-Institut für Kohlenforschung, Kaiser-Wilhelm-Platz 1, D-45470 Mülheim an der Ruhr, Germany. E-mail: felderhoff@mpi-muelheim.mpg.de

agitation (Fig. 1).[36] The grinding media are subjected to a series of collisions with the material being processed, facilitated by blades or arms attached to the rotating shaft. This interaction employs a combination of impact, shear, and compression forces to effectively reduce particle size and promote mechanochemical transformations. Designed to accommodate chamber volumes that can reach hundreds of liters and to operate in both sequential and batch modes, these systems are also ideal for large-scale operations.[37,38] Although these machines are extensively used in industry for the fine grinding of inorganic materials, their application for organic mechanochemical transformations remains limited, with existing studies focusing on the size reduction and depolymerization of biomass.[39–41]

Recognizing the significant potential of attritor mills for sustainable solvent-free co-crystal synthesis through mechanical forces, we hereby report our efforts to produce IBU:NIC co-crystals using this device. Since attritor mills can operate in sequential, continuous and batch modes, we have also conducted initial experiments to explore the potential transition from a batch process to sequential operation.

Results and discussion

Optimization of co-crystal synthesis in attritor mill

To achieve maximum efficiency in attritor mills, several operational parameters must be controlled and optimized, including for example the selection of grinding media, milling time, and rotational speed. For instance, the rotational speed plays a crucial role in determining the intensity of the grinding action, with higher speeds resulting in finer particle sizes, but leading to increased heat generation within the mill.[42–44] Initial experiments for the IBU:NIC co-crystal synthesis were carried out using a horizontal attritor mill. An equimolar amount of IBU and NIC (total weight 65 g) was placed into a 1 L reactor along with stainless steel milling balls ($d = 5$ mm, total weight 2350 g), resulting in a ball-to-powder ratio (BPR) of approximately 36. The material was processed at 500 rpm and samples were taken every 10 min to monitor the progress of the reaction. At a rotational speed of 500 rpm, Differential Scanning Calorimetry (DSC) measurements indicated full conversion of IBU and NIC after just 10 min into the desired co-crystal, which exhibited a characteristic melting endotherm at 90–92 °C (Fig. 2). Powder X-ray Diffraction (PXRD) analysis confirmed the formation of the co-crystal product, as evidenced by the distinct reflection at 3.1 2θ (Fig. 3). However, the PXRD pattern also revealed the presence of residual IBU, which exhibited a characteristic reflection at 6.1 2θ and was still detected even after 30 min of milling (Fig. 3). Consequently, the reaction was repeated and the energy input increased by setting the rotational speed to 800 rpm. Initially, similar outcomes were observed, with DSC measurements indicating full conversion after 10 min (Fig. 4). Nevertheless, also in this case PXRD analysis continued to detect residual IBU. To our delight, extending the reaction time to 30 min at 800 rpm resulted in complete conversion of the remaining starting materials into the desired IBU:NIC co-crystal (Fig. 5). After grinding out the co-
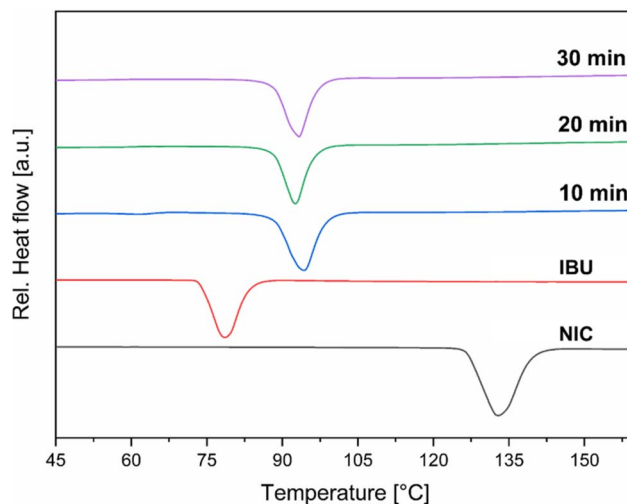

Fig. 2 DSC thermogram, showing NIC (black, m.p.: 130–132 °C), IBU (red, m.p.: 75–77 °C), and the reaction mixture after 10 min (blue), 20 min (green), and 30 min (purple) of milling at 500 rpm in attritor mill (IBU:NIC co-crystal, m.p.: 90–92 °C).

crystal and collecting the product through the outlet at the bottom of the reactor, where the grinding material was retained by an internal sieve, 99% of the co-crystal product was successfully recovered.

Assessment of material degradation and trace metal impurity accumulation in attritor mill sequential batch processing

When transitioning from a batch operation to a continuous or sequential process, it is essential to have a thorough understanding of process dynamics to prevent material accumulation at various points in the system.[45,46] Such accumulation can disrupt the intended mass flow and potentially lead to blockages. Furthermore, impurities formed during operation may
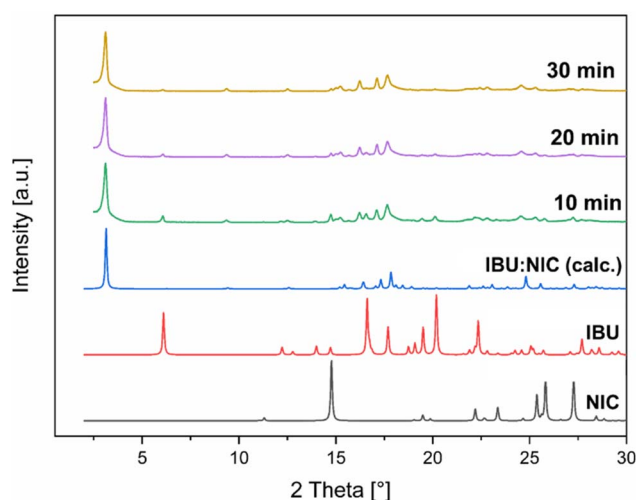

Fig. 3 PXRD pattern of NIC (black), IBU (red), calculated IBU:NIC co-crystal (blue), and of the reaction mixture after 10 min (green), 20 min (purple), 30 min (yellow) of milling at 500 rpm in attritor mill.
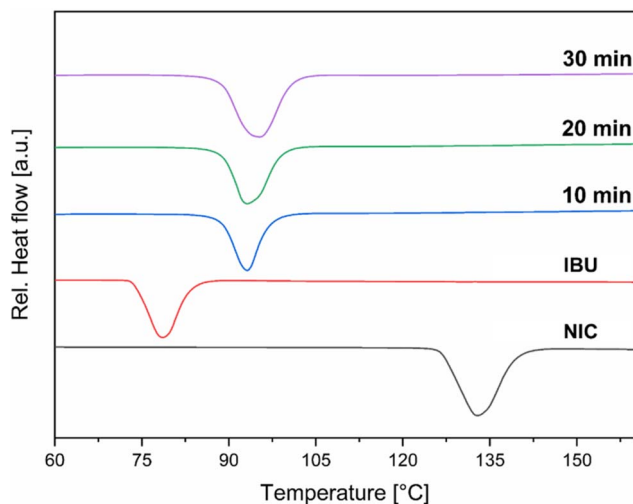
Fig. 4 DSC thermogram, showing NIC (black, m.p.: 130–132 °C), IBU (red, m.p.: 75–77 °C), and the reaction mixture after 10 min (blue), 20 min (green), and 30 min (purple) of milling at 800 rpm in attritor mill (IBU:NIC co-crystal, m.p.: 90–92 °C).
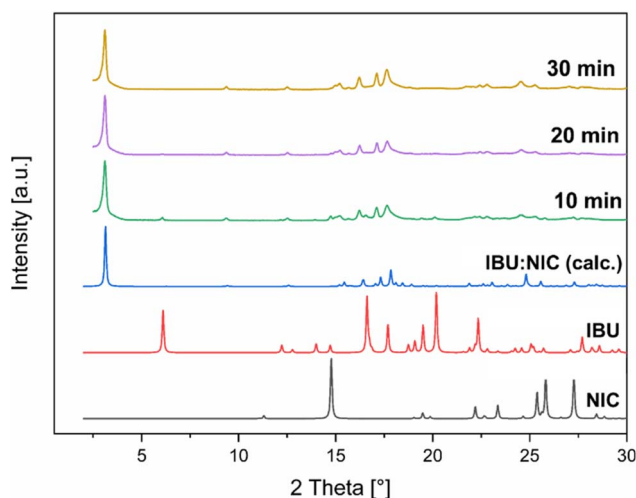
Table 1 Trace metal content analysis after each cycle for milling at 800 rpm in an attritor mill determined by ICP-OES

Sample/cycle	Al (ppm)	Cr (ppm)	Co (ppm)	Fe (ppm)	Ni (ppm)
Cycle 1	110.0	6.6	13.6	96.0	9.5
Cycle 2	34.4	6.1	11.7	70.0	8.0
Cycle 3	61.2	4.5	16.4	119.8	12.4
Cycle 4	22.1	2.9	5.8	48.9	4.6
Cycle 5	16.2	2.7	7.0	52.7	4.6
Cycle 6	73.2	3.2	13.4	120.7	10.7
Cycle 7	25.8	6.5	13.8	95.9	11.0
Cycle 8	14.7	6.0	8.7	65.4	7.4

cycle, the product was manually removed without cleaning the machine, allowing residues to remain in the reactor. Subsequently, a new milling cycle was initiated and this procedure was repeated for a total of eight cycles. Inductively Coupled Plasma Optical Emission Spectroscopy (ICP-OES) measurements were conducted for each cycle to quantify trace metal impurities from aluminium, chromium, cobalt, iron, and nickel (Table 1).

In general, the highest trace metal concentrations were observed for iron, as expected due to the high iron content in stainless steel reactor and grinding media. An interesting observation is that the amounts of trace metals did not increase with the number of cycles and no clear trend established over time for any specific element. Moreover, no degradation products could be detected when the reaction mixtures were analyzed after several cycles by PXRD (Fig. 6). This suggests that the co-crystal synthesis process in sequential batch processing can produce products without a significant risk of impurity accumulation over time. Considering that the reactor can be loaded from the top and the product can be recovered from the

Fig. 5 PXRD pattern of NIC (black), IBU (red), calculated IBU:NIC co-crystal (blue), and of the reaction mixture after 10 min (green), 20 min (purple), 30 min (yellow) of milling at 800 rpm in attritor mill.

accumulate in these specific areas of the machinery, compromising the purity of the final product. This concern is particularly relevant in mechanochemistry, where trace metals can arise from abrasion. Moreover, chemicals that remain in the reactor beyond the planned reaction time can degrade and form potentially harmful side products. Therefore, it was investigated whether residual material in the attritor mill negatively influences co-crystal purity and contribute to increased concentration of trace metal impurities in the product. As part of this investigation, we simulated a continuous process in the attritor mill by performing sequential batch processes. In this set of experiments, the machine was filled with IBU and NIC starting materials and operated under the previously optimized conditions for 30 min at 800 rpm. Upon completion of this initial
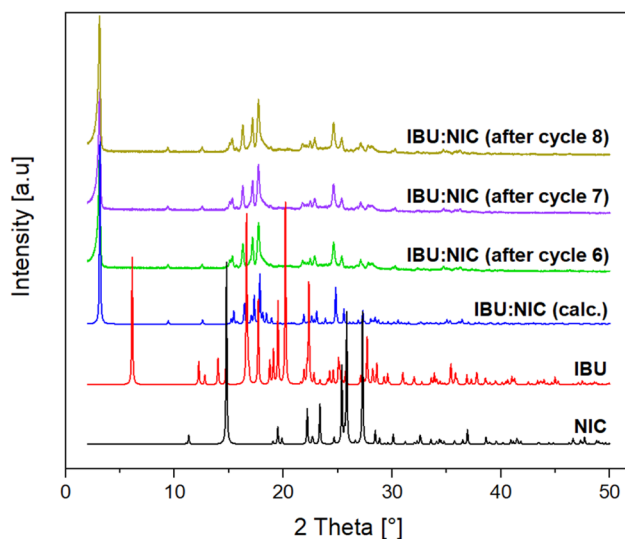

Fig. 6 PXRD pattern of NIC (black), IBU (red), calculated IBU:NIC co-crystal (blue), and of the reaction mixture after 6 cycles (green), 7 cycles (purple), 8 cycles (yellow) of sequential batch processing milling at 800 rpm in attritor mill.

bottom without removing the grinding material after each cycle, a total of 0.52 kg of the final co-crystal product was obtained within a total reaction time of 4 h. In order to facilitate the transition to a fully operational continuous process, future experiments will focus on further adapting the recovery method. This adaptation will ensure consistent removal of reaction mixtures and precise control over impurity levels during continuous operation. The observed product stability over time, along with the low trace metal content in batch processes, provides a promising foundation for this transition. Additionally, it is noteworthy that continuous co-crystallization of IBU and NIC using Hot Melt Extrusion requires elevated temperatures of 90 °C.[14,15] By applying attritor milling technology to this process, it may be possible to develop a sequential process that operates at room temperature. This would further enhance the sustainability profile by reducing the required energy input and lowering CO_2 emissions associated with heating.

Compared to the co-crystallization processes facilitated by other milling technologies, the attritor milling process in this study achieved either the same or greater recovery of IBU:NIC co-crystals (99% for attritor and drum mills[35] versus 81–94% for eccentric vibratory mills[34]) with a shorter reaction time (30 min for attritor mill versus 90 min for drum mill versus 60–120 min for eccentric vibratory mills). Moreover, the trace metal impurities detected after the attritor milling process for all measured elements (aluminum, chromium, cobalt, iron, and nickel) were lower than those observed in the eccentric vibratory mills, but higher than those in the drum mill. For example, the highest measured iron concentration was 772.2 ppm in eccentric vibratory mills, compared to 120.7 ppm in the attritor mill and 65.6 ppm in the drum mill. Therefore, trace metal values obtained in the attritor mill were below the ICH Q3D guidelines,[47] as discussed in earlier studies.[34] Additionally, it is worth noting that no additional solvent for liquid-assisted grinding was required to achieve full conversion into the desired co-crystal in the attritor mill.

Conclusions

In summary, we developed a solvent-free mechanochemical process for the synthesis of IBU:NIC co-crystals using attritor milling technology. The formation of the desired product was fast and full conversion of the starting materials was observed after just 30 min of milling at 800 rpm. By filtering the milling balls through a coarse sieve, we achieved a recovery of 99% of the co-crystal product, highlighting the straightforward workup process. The high purity achieved after this workup was confirmed by PXRD analysis. Moreover, the attritor mill was operated under sequential batch processing for 8 cycles to determine whether trace metal impurities or degradation products accumulate in the reactor system. We found that the amounts of trace metals did not increase with the number of cycles, and no additional degradation products could be detected by PXRD. Our work demonstrates the potential of utilizing attritor mills for the sustainable synthesis of pharmaceutical co-crystals.

Experimental

Materials and methods

Chemicals. *rac*-Ibuprofen (CAS: 15687-27-1) was supplied by BASF Pharma Solutions. Nicotinamide (≥98%, CAS: 98-92-0) was obtained from Alfa Aesar.

PXRD. PXRD analyses were conducted using a STOE Powder Diffraction System. This equipment included a sealed long-fine-focus Cu-tube operating at 40 kV and 40 mA, along with a short collimator and a curved Ge (111) monochromator to produce pure Cu Kα1 (λ = 1.54056 Å) radiation. Detection was accomplished using a linear position-sensitive detector (PSD) filled with a mixture of methane and argon (90 : 10). Samples were placed into borosilicate glass capillaries (d = 0.7 mm) and measured over the range of 2° to 50° (2θ) at a scanning rate of 60 s per step. STOE Win XPOW V3.05 software from STOE & Cie GmbH and Origin 2019b from OriginLab Corporation were used for data processing.

DSC. DSC analyses were performed using a METTLER TOLEDO DSC820 instrument with a heating rate set at 5 °C min^{-1}. Samples were prepared by placing the material into a standard aluminum crucible (40 μL), which was then sealed with an aluminum lid using a METTLER TOLEDO stamping device. The data were processed utilizing STARe software from METTLER TOLEDO and Origin 2019b from OriginLab Corporation.

ICP-OES. ICP-OES measurements were carried out on a SPECTROGREEN DSOI instrument, which was equipped with UVPlus optics covering a wavelength range of 165–770 nm and featured optimized Rowland Circle Alignment, operating in crossflow mode. For sample preparation, the material was dissolved in a mixture consisting of 2.5 mL of 67% HNO_3 and 7.5 mL of 37% HCl under an argon atmosphere in an Anton Paar Multiwave 5000 system. The samples were initially heated to 90 °C, followed by an increase in temperature to 180 °C. After cooling to room temperature, the resulting solution was transferred into pre-weighed centrifuge tubes and diluted with deionized water to a final volume of 50 mL. Various amounts of Berndkraft commercial reference solutions (1 g L^{-1}) were prepared as standard solutions and brought up to a total volume of 50 mL.

Synthetic procedures

General procedure for synthesis of IBU:NIC co-crystals in attritor mill. The 1 L stainless steel reactor of the attritor mill (Simoloyer CM01 from Zoz GmbH) was charged with an equimolar amount of *rac*-ibuprofen (40.8 g, 198 mmol) and nicotinamide (24.2 g, 198 mmol). Stainless steel balls (d = 5 mm, ρ = 6.7 g cm^{-3}, total weight 2350 g) were added, resulting in a filling rate of 36%. The reaction mixture was milled at room temperature at 800 rpm for 30 min. After completion of the reaction, as monitored by DSC and PXRD measurements, the IBU:NIC co-crystal was recovered through the outlet at the bottom of the reactor, while the grinding media was held back by an internal sieve (64.0 g, 195 mmol, 99%).

For sequential batch processing in the attritor, the material was processed after each cycle for 100 s at 800 rpm and

subsequently for 20 s at 400 rpm, before being extracted manually through the outlet at the bottom of the reactor.

Data availability

All experimental and characterization data, along with the experimental procedures, are available in the published article.

Author contributions

J.-H. S. drafted the original manuscript and contributed to data analysis. F. W. and S. T. performed experiments and conducted data analysis. M. F. provided project supervision and guidance. All authors contributed to the review and editing of the final manuscript.

Conflicts of interest

There are no conflicts to declare.

Acknowledgements

Notes and references

1 M. Guo, X. Sun, J. Chen and T. Cai, *Acta Pharm. Sin. B*, 2021, **11**, 2537.

2 M. K. Corpinot and D.-K. Bučar, *Cryst. Growth Des.*, 2019, **19**, 1426.

3 J. W. Steed, *Trends Pharmacol. Sci.*, 2013, **34**, 185.

4 K. Grzybowska, A. Grzybowski, J. Knapik-Kowalczuk, K. Chmiel, K. Woyna-Orlewicz, J. Szafraniec-Szczęsny, A. Antosik-Rogóż, R. Jachowicz, K. Kowalska-Szojda, P. Lodowski and M. Paluch, *Mol. Pharmaceutics*, 2020, **17**, 3087.

5 P. H. Sidwadkar, N. H. Salunkhe, K. K. Mali, V. B. Metkari and D. P. Bidye, *Futur. J. Pharm. Sci.*, 2023, **9**, 70.

6 M. Guerain, Y. Guinet, N. T. Correia, L. Paccou, F. Danède and A. Hédoux, *Int. J. Pharm.*, 2020, **584**, 119454.

7 M. Singh, H. Barua, V. G. S. S. Jyothi, M. R. Dhondale, A. G. Nambiar, A. K. Agrawal, P. Kumar, N. R. Shastri and D. Kumar, *Pharmaceutics*, 2023, **15**, 1161.

8 K. T. Savjani, A. K. Gajjar and J. K. Savjani, *ISRN Pharm.*, 2012, **2012**, 195727.

9 I. Sopyan, B. Alvin, K. S. Insan Sunan, N. H. S. Cikra Ikhda and S. Megantara, *Int. J. Appl. Pharm.*, 2021, **13**, 43.

10 Y. Yuliandra, E. Zaini, S. Syofyan, W. Pratiwi, L. N. Putri, Y. S. Pratiwi and H. Arifin, *Sci. Pharm.*, 2018, **86**, 23.

11 T. Kitak, A. Dumičić, O. Planinšek, R. Šibanc and S. Srčič, *Molecules*, 2015, **20**, 21549.

12 J. Irvine, A. Afrose and N. Islam, *Drug Dev. Ind. Pharm.*, 2018, **44**, 173.

13 S. Ishihara, Y. Hattori, M. Otsuka and T. Sasaki, *Crystals*, 2020, **10**, 760.

14 R. S. Dhumal, A. L. Kelly, P. York, P. D. Coates and A. Paradkar, *Pharm. Res.*, 2010, **27**, 2725.

15 M. Karimi-Jafari, A. Ziaee, J. Iqbal, E. O'Reilly, D. Croker and G. Walker, *Int. J. Pharm.*, 2019, **566**, 745.

16 M. Karimi-Jafari, R. Soto, A. B. Albadarin, D. Croker and G. Walker, *Int. J. Pharm.*, 2021, **601**, 120555.

17 A. L. Kelly, T. Gough, R. S. Dhumal, S. A. Halsey and A. Paradkar, *Int. J. Pharm.*, 2012, **426**, 15.

18 S. N. Madanayake, A. Manipura, R. Thakuria and N. M. Adassooriya, *Org. Process Res. Dev.*, 2023, **27**, 409.

19 E. Skorupska, S. Kaźmierski and M. J. Potrzebowski, *Mol. Pharmaceutics*, 2017, **14**, 1800.

20 N. Fantozzi, J.-N. Volle, A. Porcheddu, D. Virieux, F. García and E. Colacino, *Chem. Soc. Rev.*, 2023, **52**, 6680.

21 E. Colacino and F. Garcia, *Mechanochemistry and Emerging Technologies for Sustainable Chemical Manufacturing*, CRC Press, Boca Raton, 2023, vol. 1.

22 O. Galant, G. Cerfeda, A. S. McCalmont, S. L. James, A. Porcheddu, F. Delogu, D. E. Crawford, E. Colacino and S. Spatari, *ACS Sustain. Chem. Eng.*, 2022, **10**, 1430.

23 M. Solares-Briones, G. Coyote-Dotor, J. C. Páez-Franco, M. R. Zermeño-Ortega, C. M. de la O Contreras, D. Canseco-González, A. Avila-Sorrosa, D. Morales-Morales and J. M. Germán-Acacio, *Pharmaceutics*, 2021, **13**, 790.

24 S. L. James, C. J. Adams, C. Bolm, D. Braga, P. Collier, T. Friščić, F. Grepioni, K. D. Harris, G. Hyett, W. Jones, A. Krebs, J. Mack, L. Maini, A. G. Orpen, I. P. Parkin, W. C. Shearouse, J. W. Steed and D. C. Waddell, *Chem. Soc. Rev.*, 2012, **41**, 413.

25 S. Pagola, *Crystals*, 2023, **13**, 124.

26 K. J. Ardila-Fierro and J. G. Hernández, *ChemSusChem*, 2021, **14**, 2145.

27 D. J. C. Constable, C. Jimenez-Gonzalez and R. K. Henderson, *Org. Process Res. Dev.*, 2007, **11**, 133.

28 C. S. Slater, M. J. Savelski, W. A. Carole and D. J. C. Constable, in *Green Chemistry in the Pharmaceutical Industry*, ed. P. J. Dunn, A. S. Wells and M. T. Williams, Wiley-VCH, Weinheim, 2010, p. 49.

29 J. Alic, M. C. Schlegel, F. Emmerling and T. Stolar, *Angew. Chem., Int. Ed.*, 2024, **63**, e202414745.

30 F. Gomollón-Bel, *ACS Cent. Sci.*, 2022, **8**, 1474.

31 J. F. Reynes, V. Isoni and F. García, *Angew. Chem., Int. Ed.*, 2023, **62**, e202300819.

32 E. Colacino, V. Isoni, D. Crawford and F. García, *Trends Chem.*, 2021, **3**, 335.

33 M. Felderhoff and J.-H. Schöbel, in *Reference Module in Chemistry, Molecular Sciences and Chemical Engineering*, Elsevier, 2024.

34 A. Bodach, A. Portet, F. Winkelmann, B. Herrmann, F. Gallou, E. Ponnusamy, D. Virieux, E. Colacino and M. Felderhoff, *ChemSusChem*, 2024, **17**, e202301220.

35 J.-H. Schöbel, F. Winkelmann, J. Bicker and M. Felderhoff, *RSC Mechanochem.*, 2025, **2**, 224.

36 C. Suryanarayana, *Prog. Mater. Sci.*, 2001, **46**, 1.

37 P. Baláž, in *Mechanochemistry in Nanoscience and Minerals Engineering*, Springer Berlin, 2008, p. 103.

38 F. Hadef and A. Otmani, in *Handbook of Mechanical Nanostructuring*, ed. M. Aliofkhazraei, Wiley-VCH, Weinheim, 2015, vol. 1, pp. 263.

39 R. Rajkhowa, L. Wang, J. Kanwar and X. Wang, *Powder Technol.*, 2009, **191**, 155.

40 R. G. Blair, in *Production of Biofuels and Chemicals with Ultrasound*, ed. Z. Fang, J. R. L. Smith and X. Qi, Springer Netherlands, Dordrecht, 2015, pp. 269.

41 S. M. Hick, C. Griebel, D. T. Restrepo, J. H. Truitt, E. J. Buker, C. Bylda and R. G. Blair, *Green Chem.*, 2010, **12**, 468.

42 T. M. Cook and T. H. Courtney, *Metall. Mater. Trans. A*, 1995, **26**, 2389.

43 R. W. Rydin, D. Maurice and T. H. Courtney, *Metall. Trans. A*, 1993, **24**, 175.

44 X. Zhao and L. Shaw, *Metall. Mater. Trans. A*, 2017, **48**, 4324.

45 Y. J. Zhang, H. Yang, R. Li, Q. Chen, Q. C. Sun and P. Kong, *Powder Technol.*, 2019, **355**, 333.

46 C. Hu, *J. Flow Chem.*, 2021, **11**, 243.

47 A. Teasdale and S. Thompson, in *ICH Quality Guidelines*, 2017, pp. 233.

48 https://www.mechanochemistry.eu, accessed October 23, 2024.